

# Short Gamma Ray Bursts and their Afterglow Signatures in Dense Stellar Systems

Rion K. Parsons<sup>1</sup>, Enrico Ramirez-Ruiz<sup>1</sup> and William H. Lee<sup>2</sup>

## ABSTRACT

The hypothesis that short GRBs arise from the coalescence of binary compact stars has recently gained support. With this comes the expectation that the afterglow should bear the characteristic signature of a tenuous intergalactic medium (IGM). However, fits to the observational data suggest that some detected afterglows arise in relatively dense gaseous environments rather than in the low density IGM. Here we show that considering the effect of red giant winds in the core of a star cluster may resolve this paradox if short GRB progenitors are contained in such an environment and close encounters rather than pure gravitational wave emission brings the compact objects together. Clear confirmation is provided here of the important notion that the morphology and visibility of short gamma-ray burst remnants are determined largely by the state of the gas in the cluster's core.

*Subject headings:* stars: neutron — shock waves — globular clusters: general — gamma rays: bursts — hydrodynamics — stars: winds

## 1. Introduction

Although they were discovered roughly forty years ago (Klebesadel, Strong & Olson 1973), Short  $\gamma$ -Ray Bursts (SGRBs) are still a mystery. All that can confidently be said is that they involve compact objects and highly relativistic dynamics. The most widely favored and conventional possibility is that they are produced by the coalescence of compact object binaries involving neutron stars and/or black holes, although other alternatives should also be considered (see e.g. Nakar 2007; Lee & Ramirez-Ruiz 2007, for reviews). Such systems, which are known to exist (Hulse & Taylor 1975; Burgay et al. 2003), are driven to coalesce

---

<sup>1</sup>Department of Astronomy and Astrophysics, University of California, Santa Cruz, CA 95064

<sup>2</sup>Instituto de Astronomía, Universidad Nacional Autónoma de México, Apdo. Postal 70-264, Cd. Universitaria, México D.F. 04510

by energy and angular momentum losses to gravitational radiation. In this scenario, the compact binary would take hundreds of millions of years to spiral together, and could by then (especially if given a kick velocity on formation) have moved many kilo-parsecs from the site of its birth (Fryer et al. 1999; Bloom et al. 1999). However, fits to the observational data suggest that some detected afterglows (Berger 2007; Nakar 2007; Panaitescu 2006; Nysewander et al. 2008) arise in relatively dense gaseous environments rather than in the low density Intergalactic Medium (IGM). We must therefore remain aware of other possibilities. It may be wrong, for instance, to suppose that the binary is formed in isolation, since it could instead be the result of an encounter in a dense stellar system.

Most stars in the Universe never interact strongly with others, at least during their adult life, after they have left the interstellar gas cloud in which they were born. However, there are various *dense stellar systems* such as star clusters and galactic centers, where stars are sufficiently close to their neighbors to make encounters significantly more likely. To get a sense of how crowded such a region is, consider the contents of the inner core of a Globular Cluster (GC). While in the Solar neighborhood the typical distance between individual stars is more than 1 pc, a sphere with a radius of 0.1 pc around the core of a GC contains over a hundred thousand, if not millions, of solar masses in stars following tight orbits about the nucleus. The stellar density is therefore more than a million times higher than that in the neighborhood of our Sun. In such environments, it is unavoidable that many single and binary stars will undergo close encounters and even physical collisions within their lifetimes. Indeed, it is thought that this type of interaction can lead to the formation of blue stragglers (Glebbeek, Pols & Hurley 2008), and possibly intermediate mass black holes (Portegies Zwart et al. 2004). It is in these environments, called dense stellar systems, that a compact object binary can be formed by two- and three-body encounters (Grindlay, Portegies-Zwart & McMillan 2006). The subsequent merger, or possibly direct collisions of compact objects (Lee & Ramirez-Ruiz 2007), can produce a SGRB, and the resulting afterglow could then at least in part be due to the interaction of the relativistic ejecta with the stellar winds of the cluster members. Due to the large stellar density in the star cluster core, the interaction of the external shock can take place with a denser external medium than that of the IGM. Much of the effort herein will be dedicated to determining the state of the circumburst material in the cores of GCs, and describe how this external matter can affect the observable burst and afterglow characteristics.

## 2. SGRBs from Dense Stellar Systems

First, we assume that different types of stellar objects are distributed homogeneously in a spherical core of radius  $r_c = 0.1r_{c,-1}$  pc, within which the number density,  $n_c$ , and stellar velocity dispersion,  $\sigma_c$ , are constant. The gas density in the cores of GCs depends on the various types of stellar members that populate their interiors. In a typical cluster, winds from red giant stars tend to have the greatest effect on the core’s gas density despite being significantly outnumbered by other stellar types. These winds are typically slow-moving and dense, with velocities on the order of  $v_w = 10v_{w,1}$  km s<sup>-1</sup> and mass loss rates between  $10^{-7}$  and  $10^{-6}$  M<sub>⊙</sub> yr<sup>-1</sup>. In a steady, spherically symmetric solution, the electron density is

$$n_w(r) \approx 3 \times 10^3 r_{16}^{-2} v_{w,1}^{-1} \dot{M}_{w,-7} \mu_e^{-1} \text{ cm}^{-3}, \quad (1)$$

where  $\mu_e \sim 2$  in a Helium gas,  $r = 10^{16} r_{16}$  cm and  $\dot{M}_w = 10^{-7} \dot{M}_{w,-7}$  M<sub>⊙</sub> yr<sup>-1</sup>. The inner core of a GC contains  $N_* = 10^2 N_{*,2}$  red giants, and so their mean separation is

$$r_{\perp} = 6.4 \times 10^{16} N_{*,2}^{-1/3} r_{c,-1} \text{ cm}. \quad (2)$$

We can thus estimate a minimum average density  $n_{\perp}$  in the cores of GCs in the absence of gas retention as:

$$n_{\perp} \sim n_w(r_{\perp}) = 80 N_{*,2}^{2/3} r_{c,-1}^{-2} v_{w,1}^{-1} \dot{M}_{w,-7} \mu_e^{-1} \text{ cm}^{-3}. \quad (3)$$

In this case, the SGRB would expand into a medium that is significantly denser than the IGM.

For this discussion we will assume that the blast wave is adiabatic, i.e. its energy is constant with time, and effectively spherically distributed. This means that the energy ( $E = 10^{50} E_{50}$  erg) is the *isotropic equivalent* energy as, for example, derived from the  $\gamma$ -ray output. Deceleration due to the combined stellar winds starts in earnest when about half the initial energy has been transferred to the shocked matter, i.e. when it has swept up  $\Gamma^{-1}$  times its own rest mass. The typical mass where this happens is  $M_{\text{dec}} = E/(\Gamma^2 c^2) \approx 5 \times 10^{-8} E_{51} \Gamma_2^{-2} M_{\odot}$ . In the GC core, the mass within radius  $r$  is  $\frac{4\pi}{3} \rho_{\perp} r^3$ , which gives the blast wave deceleration radius

$$r_d = 10^{16} E_{50}^{1/3} \Gamma_2^{-2/3} \left( \frac{n_{\perp}}{1 \text{ cm}^{-3}} \right)^{-1/3} \text{ cm}. \quad (4)$$

A blast wave in a GC core thus decelerates at a much smaller radius than it would in the IGM.

Under the assumption that energy conversion takes place primarily within the forward shock, the energy equation reads  $E_{\text{bw}}(t) = \psi \Gamma^2 M_{\text{bw}} c^2$ , where  $E_{\text{bw}}$  is the blast wave’s isotropic equivalent energy,  $\psi$  is a constant of order unity (Blandford & McKee 1976), and  $M_{\text{bw}}(r_{\text{bw}}) \equiv$

$4\pi \int_0^{r_{\text{bw}}} n_{\text{w}}(r)r^2 dr$  is the cumulative swept-up mass. The observed time interval during which most of the photons emitted (at a radius  $r_{\text{bw}}$ ) are received is of the order of  $r_{\text{bw}}/(4\Gamma^2 c)$  (Sari, Piran & Narayan 1998).

As usual, we assume that the dominant radiation process is synchrotron emission. If the energy in the magnetic field and electrons are taken to be a fraction  $\epsilon_{\text{B}}$  and  $\epsilon_{\text{e}}$ , respectively, of the thermal energy density, then approximating the electron energy distribution as a power law with an index  $p$ , the afterglow flux during the adiabatic expansion of the blast wave is given by

$$F_{\nu} \propto \nu^{(1-p)/2} n^{(1+p)/4} E_{\text{bw}}^p M_{\text{bw}}^{1-p} \epsilon_{\text{B}}^{(1+p)/4} \epsilon_{\text{e}}^{(p-1)} \quad (5)$$

for  $\nu_{\text{sy}} < \nu < \nu_{\text{c}}$ , and

$$F_{\nu} \propto \nu^{-p/2} n^{(p-2)/4} E_{\text{bw}}^{p-1} M_{\text{bw}}^{2-p} t^{-1} \epsilon_{\text{B}}^{(p-2)/4} \epsilon_{\text{e}}^{(p-1)} \quad (6)$$

for  $\nu_{\text{c}} < \nu$ . The above relations are valid for varying energy or density, as can be seen by considering the implicit time dependence through  $E_{\text{bw}}(t)$ ,  $n(t)$  and  $M_{\text{bw}}(t)$ .

When the dominant variations are in the circumburst matter rather than energy, one may write  $t = (c/4E)(M_{\text{bw}}r_{\text{bw}} + \int_0^{r_{\text{bw}}} r^2 n(r) dr)$ . Under this assumption, equations (5) and (6) reduce to  $F_{\nu} \propto M_{\text{bw}}^{1-p} n^{(p+1)/4}$  and  $F_{\nu} \propto M_{\text{bw}}^{2-p} t^{-1} n^{(p-2)/4}$ , respectively. As the blast wave expands into the cluster winds, strong temporal variations compared to the canonical power-law decay can thus be produced as a result of changes on the properties of the star cluster, especially the mass-loss rates of the stars and their number density. The characteristic mass scale where this takes place is  $M_{\text{bw}} \gtrsim M_{\text{dec}}$ . This phase ends when so much mass shares the energy that the  $\beta\Gamma \leq 1$ , setting a non-relativistic mass scale  $M_{\text{NR}} = E/c^2 \approx 5 \times 10^{-5} E_{50} M_{\odot}$ . Beyond this point, the event slowly changes into a classical Sedov-Taylor supernova remnant evolution.

In the absence of characteristic scales in stellar ejecta and in the ambient medium, self-similar, spherically symmetric solutions exist, and they are widely used to interpret observational data on afterglows. By contrast, the interaction of a GRB with a non-uniform medium is poorly understood. The presence of a density gradient will only affect the dynamics of the GRB when the remnant size is comparable to, or exceeds, the scale length of the gradient. Before this time, the density can be treated as approximately uniform. Thus, it is only when  $r_{\text{d}} \gtrsim r_{\perp}$  that the details of the transition are important for the dynamics. This requires

$$\frac{E_{51} v_{\text{w},1} r_{\text{c},-1} \mu_{\text{e}}}{\Gamma_{*2}^2 N_{*2}^{1/3} \dot{M}_{\text{w},-7}} \gtrsim 10^3. \quad (7)$$

A close examination of equation (7) shows that if the winds of red giants are especially weak (i.e.  $\dot{M}_{-7} < 1$ ) or the burst's energy content is large ( $E_{51} > 1$ ),  $r_{\perp}$  falls within the range of

relativistic expansion. Otherwise, this radius is sufficiently large that the interaction with the free wind of the nearest red giant is expected over the typical period of observation of afterglows.

Depending on the wind properties of the stellar members as well as their number density, however, the density structure in this region could be quite complicated as the winds of stars interact at a typical distance  $\sim r_{\perp}/2$ . Each free expanding wind encounters an inward facing shock, where the typical preshock densities are  $\sim 4n_{\perp} \sim 320\dot{M}_{w,-7}N_{*,2}^{2/3}r_{c,-1}^{-2}v_{w,1}^{-1} \text{ cm}^{-3}$ . Kinetic energy is deposited in the shocked wind region in the form of heat, with temperature  $T_{\text{shock}} = (3m_p\mu_e/16k)(\Delta v_w)^2 = 4 \times 10^3(\Delta v_w/10 \text{ km s}^{-1})^2 \text{ K}$ , where  $\Delta v_w$  is the speed of the material relative to the approaching shock.

The shock interactions between nearby stars will be radiative if the cooling distance  $r_{\text{cool}}$  satisfies the condition  $\kappa = r_{\text{cool}}/r_{\perp} < 1$ . Using the cooling distances obtained by Hartigan, Raymond & Hartmann (1987) for shocks in the low-density regime derived from self-consistent pre-ionization, plane-parallel, steady models, we obtain  $\kappa \ll 1$ . A cluster wind in this high cooling regime will have dense, cool structures between nearby stars and the SGRB blast wave could interact with them while still relativistic provided that  $r_d < r_{\perp}$ . Large-scale density inhomogeneities in the circumburst medium are, however, likely to result in distortions of the ejecta that might be more readily observed as the blast wave evolves into the non-relativistic phase.

### 3. Cluster Winds Interaction Models for SGRBs

#### 3.1. Initial Model

To build the initial model,  $N_*$  stars were randomly distributed in a three-dimensional volume such that the mean separation between stars is  $r_{\perp} \sim N_*^{1/3}r_c$ . The computational box is  $8.0 \times 10^{17} \text{ cm}$  in each dimension with the stars located within the central  $r_c \sim 6.0 \times 10^{17} \text{ cm}$ . Based on the data from M15 (Dull et al. 1997; van den Bosch et al. 2006), the number density of red giants within  $r_c$  is somewhere between 10 and 100, and for this particular simulation we set  $N_* = 10^2$ , such that  $r_{\perp} \sim 6 \times 10^{16} \text{ cm}$ . Each star was given the same effective mass loss rate  $\dot{M}_{\text{RG}} = 10^{-7} M_{\odot} \text{ yr}^{-1}$  and stellar wind speed  $v_{\text{RG}} = 10 \text{ km s}^{-1}$ . Based on  $\dot{M}_{\text{RG}}$  and  $v_{\text{RG}}$ , a spherical  $1/r^2$  wind profile was implemented for each cluster member (Figure 1). The individual density profiles were then extrapolated so that they are in ram pressure equilibrium with the closest neighbor.

### 3.2. Dynamics of SGRB Remnants

In the case depicted in Figure 1 the stellar winds of the individual members are dense enough to slow down the ejecta (for reasonable SGRB properties) to non-relativistic speeds before reaching  $r_{\perp}$ , so that we expect the blast wave evolution as we see it to take place in the free-expansion phase. This encourages us to present a detailed account of resulting dynamics of the remnants within a dense stellar system following the onset of the non-relativistic phase. Common to all calculations is the initiation of the SGRB explosion as two identical blobs expanding in opposite directions into the circumburst medium. Calculations were done in three dimensions using the PPM adaptive mesh refinement code FLASH (ver 2.5). The blobs and the circumburst medium are modeled as a cold ideal gas with  $\gamma = 5/3$ . The numerical domain is a unprolonged cylinder in which the ejecta moves along the  $y$ -axis. In the inner region of each of the pancakes, the ejecta mass,  $M_j$  is distributed uniformly and for all runs we have used  $\Gamma_j = 2$ ,  $\Delta r_j/r_j \sim 0.6$ ,  $\theta_j \sim 0.5$ , and  $r_j \sim r_d(\Gamma_j)$ .

Without a detailed understanding of the exact shape and energy distribution of the ejecta, we have only an approximate description of how to construct the initial conditions. However, as clearly illustrated by Ayal & Piran (2001) and Ramirez-Ruiz & MacFadyen (2008), the late time evolution of the ejecta is rather insensitive to uncertainties in the initial conditions. We have considered various initial densities, angular widths, and shapes of the collimated ejecta and found that these are indeed unimportant in determining the late morphology of the remnant. This stems from the fact that at late times the mass of the remnant is dominated by the circumburst gas, which washes out any variations in the initial conditions of the ejecta.

Detailed hydrodynamic simulations of the evolution of a GRB remnant in the GC core medium are presented in Figure 2, where the pressure contours of the expanding ejecta are plotted. As the gas collides with the external medium, a blast wave forms that propagates in the radial direction of motion and, over time, wraps around the various density discontinuities produced by the red giant stars. As it can be seen in panel (a) in Figure 2, the evolution of the blast wave suffers only minor distortions as the remnant sweeps a mass  $\sim E/c^2$ . By the time the blast wave reaches the edge of the cluster’s core, it becomes fairly distorted, though it still holds a jet-like appearance. Pronounced dimples are clearly visible in the lower portion of the blast wave showing where stars have been overtaken. Also shown in Figure 2 for comparison is the evolution of a spherical blast wave of comparable isotropic equivalent energy.

The calculations above demonstrate how the dynamical evolution of SGRB remnants in dense stellar systems depends sensitively on the stellar wind properties of the cluster members as well as their density distribution. This confirms the notion that that the morphology

and visibility of short gamma-ray burst remnants are determined largely by the state of the gas in the cluster’s core. The resulting evolution depends also fairly strongly on the properties of the GRB ejecta, especially its energy content, since it sets the non-relativistic mass scale for a particular stellar cluster. Figure 3 illustrates the dependence on energy of the remnant’s morphology, where structures similar to those described in Figure 2 are clearly seen. A bow shock forms as each blob collides with the surrounding medium, which eventually wraps around the ejecta before the two expanding shells collide to form a single structure. However, in the low energy content case (panel a) the GRB remnant decelerates much more rapidly and although initially it may be highly nonspherical, the aspect ratio approaches unity as the two blobs expand and merge before reaching the edge of the GC core at about  $2.3 \times 10^8$  seconds. Beyond this point, the evolution will follow the classical Sedov-Taylor supernova remnant solution. With higher energy content, on the other hand, deceleration to non-relativistic velocities occurs at much larger radii (panel c), and the blast wave is still moving through the core region before the two expanding shells collide to form a single structure.

#### 4. Discussion

It is evident from the above discussion that the environment in the cores of GCs is a very rich one in terms of observable consequences. Even in the simplest case of red giant stars with identical wind properties, complex behavior with multiple possible transitions in the observable part of the GRB remnant’s lifetime may be seen. Detailed, high resolution 3D simulations of a spherical GRB exploding within the core of a dense stellar environment have been presented here, which show the resulting dynamics of the remnants following the onset of the non-relativistic phase. The resulting afterglow light curve will depend fairly strongly on the properties of the system, especially the mass-loss rates of the stars and their number density with various implications. On the one hand, it implies that one cannot be too specific about the times at which we expect to see transitions in the observed emission. More constructively, if and when we do see these transitions, they can be fairly constraining on the properties of the birth sites. If we continue to see the population of afterglows dominated by high inferred densities when compared to the IGM, this is support for blast waves in dense stellar systems, i.e. support for the origin of SGRBs from dynamically formed compact binaries or collisions.

Stars in a dense stellar system interact with each other, both through their ionizing radiation and through mass, momentum and energy transfer in their winds. Mass loss leads to recycling of matter into the cluster wind gas, often with chemical enrichment. The

task of finding useful progenitor diagnostics is simplified if the pre-burst evolution leads to a significantly enhanced gas density in the immediate neighborhood of the burst. The detection of absorption signatures associated with the SGRB environment would provide important clues about the triggering mechanism and the progenitor.

ER-R was supported in part by the David and Lucile Packard Foundation, NASA: Swift NNX08AN88G and DOE SciDAC: DE-FC02-01ER41176. WHL acknowledges financial support from CONACyT (45845E) and PAPIIT (IN113007) and thanks the Department of Astronomy and Astrophysics, UC-Santa Cruz for hospitality.

## REFERENCES

- Ayal, S., & Piran, T. 2001, *ApJ*, 555, 23
- Berger, E. 2007, *ApJ*, 670, 1254
- Blandford, R. D., McKee, C. F. 1976, *Phys. Fl.*, 19, 1130
- Bloom, J. S., Sigurdsson, S., & Pols, O. R. 1999, *MNRAS*, 305, 763
- Burgay, M. et al. 2003, *Nature*, 426, 531
- Dull, J.D., Cohn, H.N., Lugger, P.M., Murphy, B.W., Seitzer, P.O., Callanan, P.J., Rutten, R.G.M., Charpes, P.A., 1997, *ApJ*, 481, 267
- Fryer, C. L., Woosley, S. E., & Hartmann, D. H. 1999, *ApJ*, 526, 152
- Glebbeeck, E., Pols, O.R., Hurley, J.R. 2008, *A&A*, 488, 1007
- Grindlay, J., Portegies Zwart, S., McMillan, S.L.W. 2006, *Nature Phys.*, 2, 116
- Hartigan, P., Raymond, J., Hartmann, L. 1987, *ApJ*, 316, 323
- Hulse, R.A., Taylor, J.H. 1975, *ApJ*, 195, L51
- Klebesadel, R.W., Strong, I.B. Olson, R.A. 1973, *ApJ*, 182, L85
- Lee, W.H., Ramirez-Ruiz, E. 2007, *New. J. Phys*, 9, 17
- Nakar, E. 2007, *Phys. Rep.*, 442, 166
- Nysewander, M., Fruchter, A. S., & Pe'er, A. 2008, arXiv:0806.3607

Panaitescu, A. 2006, MNRAS, 367, L42

Portegies Zwart, S.F., Baumgardt, H., Hut, P., Makino, J., McMillan, S.L.W. 2004, Nature, 428, 724

Ramirez-Ruiz, E., & MacFadyen, A. I. 2008, arXiv:0808.3448

Sari, R., Piran, T., Narayan, R. 1998, ApJ, 497, L17

van den Bosch, R., de Zeeuw, T., Gebhardt, K., Noyola, E., van de Ven, G. 2006, ApJ, 641, 852

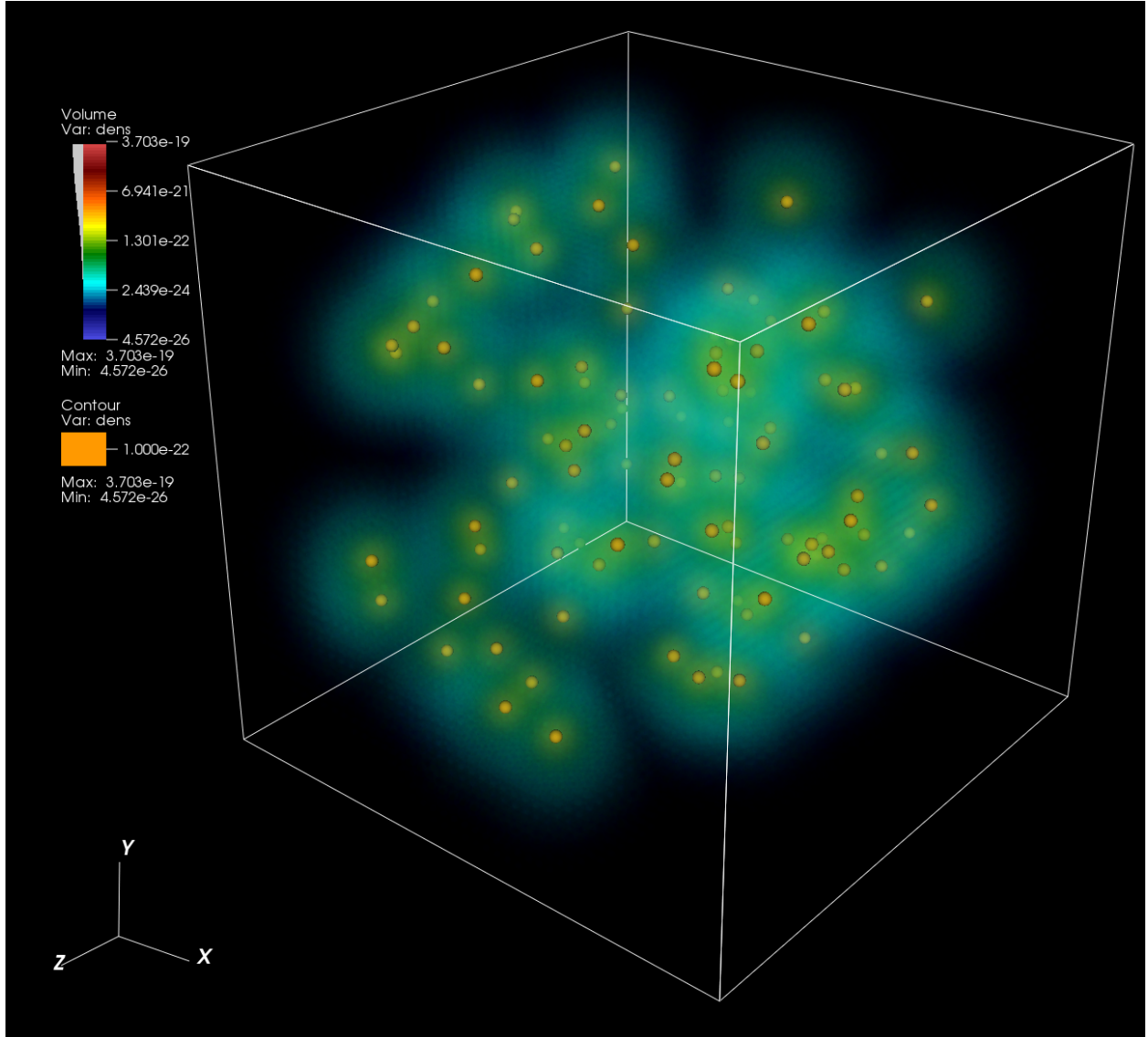


Fig. 1.— Simulated red giant stars within the GC core. Each star is surrounded by a  $1/r^2$  density profile, and is in ram pressure equilibrium with neighboring stars. The yellow surface is a contour of constant density (in  $M_{\odot}c^{-3}s^{-3}$  units) around the star, and is not representative of the actual (unresolved) stellar radius. The size of the computational domain is  $(0.2 \text{ pc})^3$ .

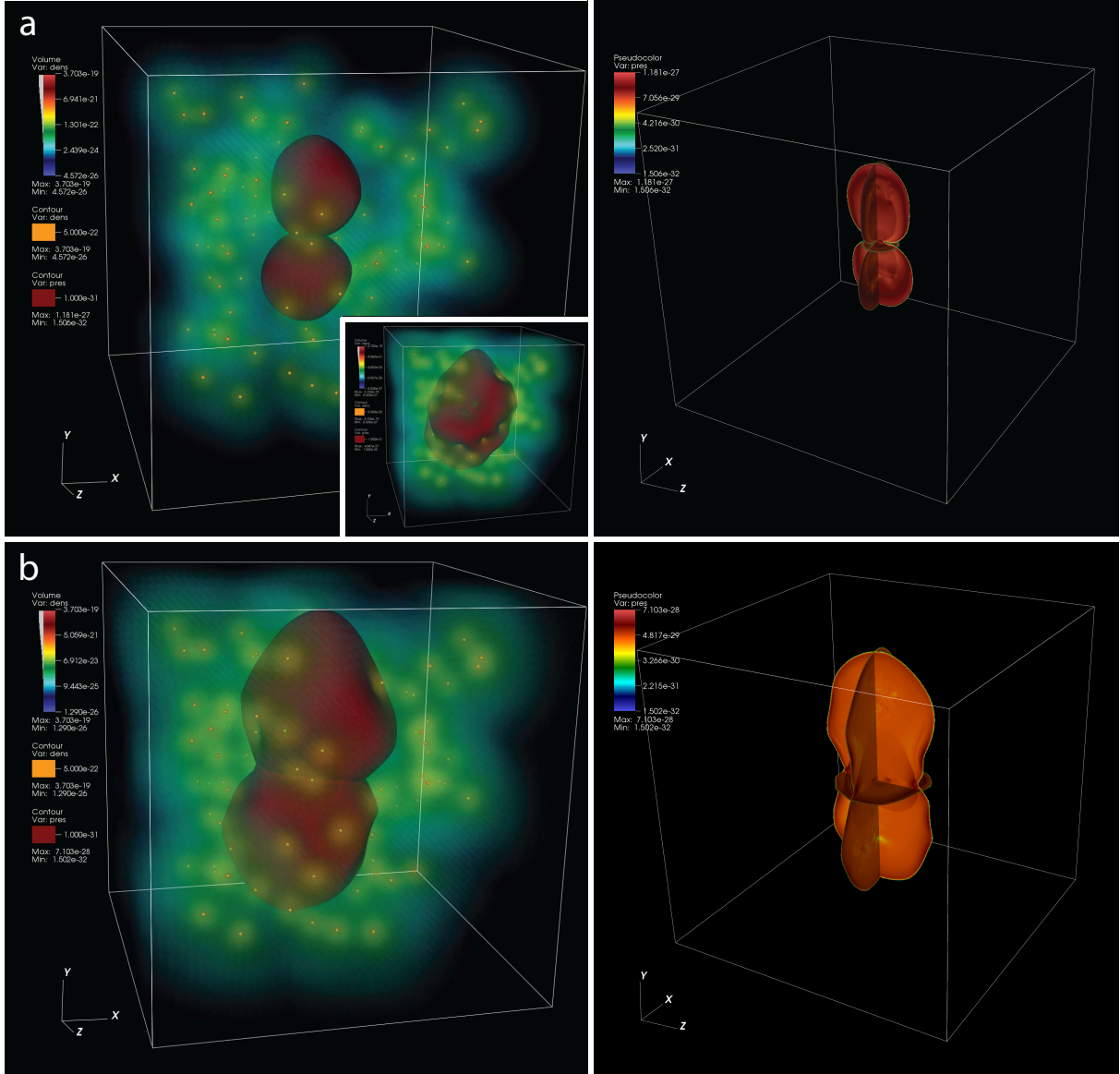


Fig. 2.— Morphology of the SGRB remnant  $4.8 \times 10^7$  (a, top row) and  $1.9 \times 10^8$  (b, bottom row) seconds after explosion. In the left panels, the pressure isosurface (in units of  $M_{\odot}c^{-1}s^{-3}$ ) is located at the outer boundary of the blast wave, and yellow/green/blue shading shows the density profile around the stars (in  $M_{\odot}c^{-3}s^{-3}$  units). In the early stages, the blast wave remains largely undisturbed. The size of the computational domain is  $(0.2 \text{ pc})^3$ , and calculations were carried out in cartesian coordinates in three dimensions with six levels of refinement. The pressure slices in the right column show the region interior to the blast wave for each case. *Inset panel:* Behavior of a spherical explosion with a comparable isotropic equivalent energy  $E_{\Omega} = 5 \times 10^{48}$  erg. The initial high pressure region in this case is a sphere in which the ejecta mass, and the thermal energy are initially uniformly distributed.

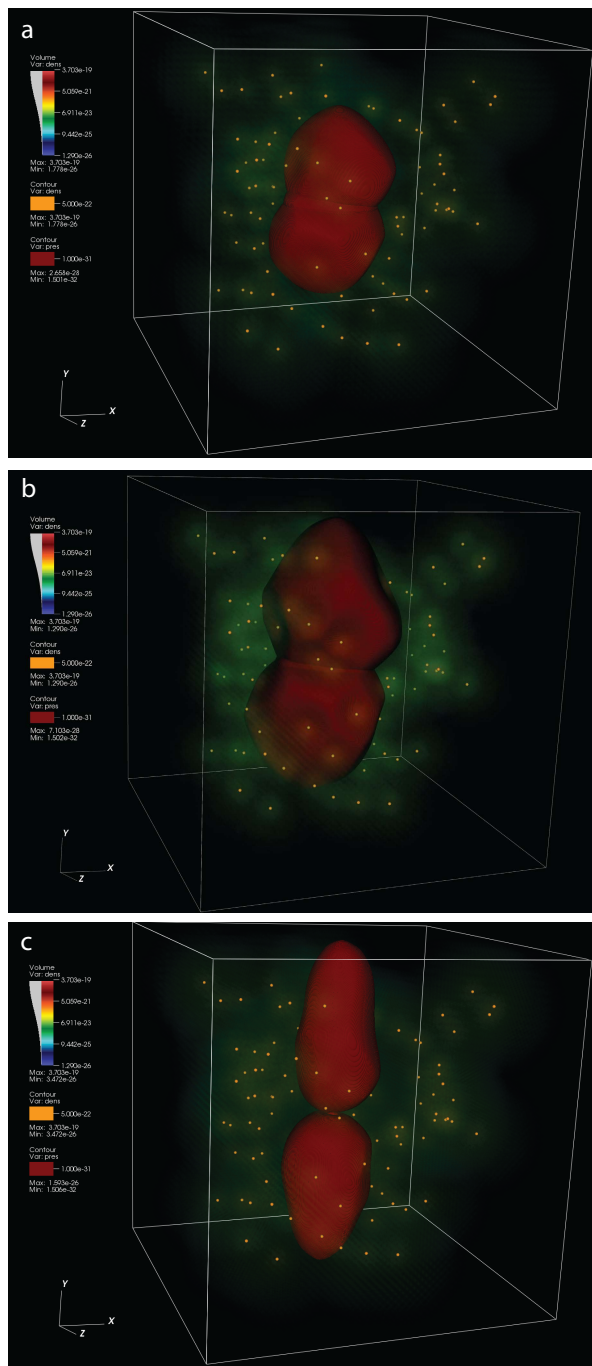


Fig. 3.— The evolution of a SGRB remnant with varying energy at  $t = 2.3 \times 10^8$ ,  $10^8$  and  $4.4 \times 10^7$  seconds (panels a,b and c, respectively). Shown are 3D pressure isosurfaces in normalized units ( $M_{\odot}c^{-1}s^{-3}$ ) for calculations with  $E_{\Omega} = 5 \times 10^{47}$ ,  $5 \times 10^{48}$  and  $5 \times 10^{49}$  erg (panels a,b and c, respectively). The blast wave has reached the edge of the core radius, at which point it has become extremely distorted. Pronounced dimples are clearly visible in the lower portion of the blast wave showing where stars have been overtaken.